

Evaluation of Performance of an Industrial Gas Sweetening Plant by Application of Sequential Modular and Simultaneous Modular Methods

F. Bimakr, M. Baniadam, and J. Fathikalajahi*
Chemical & Petroleum Engineering Department,
Shiraz University, Shiraz, Iran

Original scientific paper
Received: September 9, 2007
Accepted: February 6, 2008

In this study the simultaneous-modular and sequential modular methods are used to predict performance of desorption and absorption columns in the loop of an industrial sweetening plant. Mathematical model of absorption and desorption cycle for acid gases in methyldiethanolamine has been developed. This model is based on mass and energy balance and takes into account the chemical interactions between solvent and gases. Application of the simultaneous-modular method to model of the plant provides 31 equations with 31 unknowns. Simultaneous solution of these equations presents details of operating conditions on each section of the process. In the sequential modular method, the calculations have been carried out for each unit as a single module in the loop. This way, the output of each module supplies the input data to the next unit. Data of a commercial gas refinery has been used to validate the models and compare the two methods. After validating, the model effects of some parameters on the performance of the loop have been investigated.

Key words:

Steady-state flowsheeting, acid gas absorption, sweetening, process simulation

Introduction

Process simulation is the act of representing some aspects of the real world by numbers or symbols that may be easily manipulated to facilitate their study. Typically, process simulation is needed to solve problems related to process design, process analysis, process control and many other. Depending on the type of problem, different types of process simulation problems can be noticed. Obviously, each simulation is associated with a mathematical model that expresses the physical situation in terms of certain equations. The nature of these equations is closely related to the changes taking place in the process. In steady-state simulation, the mathematical model is usually represented by a set of algebraic equations, while in dynamic simulation the mathematical model is usually represented by a mixed set of algebraic equations and ordinary differential or partial equations.¹

Two distinctly different approaches exist which chemical engineers use for modeling processes: the “sequential modular approach” underlying most of the commercially available modeling systems, and the “equation-based approach”.^{2–4}

Sequential modular modeling underlies most of the flowsheet simulation programs developed since Kellogg announced their flexible flowsheeting program in 1958. In this approach, there are subrou-

tines for each unit. The flowsheeting system then solves the total process model by calling each of the unit models in turn, according to how they are wired together, iterating where necessary to converge complex process models.⁵

Calculations in each unit are performed by numerical programs written in some modules. Input of each module is the calculated outputs from previous modules. To calculate a flowsheet of interconnected units, solution procedures are applied in sequence determined by the process topology. Flowsheet decomposition techniques or equation ordering techniques determined the calculation sequence. If recycles are present, then an iteration calculation is performed where some recycle stream(s) become the tear stream(s), and a convergent sequence of guesses for them is produced by standard numerical algorithms.⁶

The developers of these unit models include all sorts of special tricks to make these computations robust. A unit model will converge when there is a solution for its underlying equations and it fails reasonably when there is not. These tricks include developing initial guesses from which the equations typically converge. There are detectors in many of these codes to discover the lack of convergence and then tests to decide what to try next to gain convergence. Each is often like a mini-expert system, containing every bit of knowledge a modeler knows and learns about such a model to make it work.

*Corresponding author: fathi@shirazu.ac.ir

Most of the code in such routines is to assure this robustness.⁵

The equation-oriented algorithms have been under development since the mid 60's (SPEEDUP by Sargent and Westerberg) but have only recently been successfully implemented in commercial simulators that have wide audience (AspenPlus 11 and subsequent releases).⁷ An equation-oriented chemical process flowsheeting system may contain many thousands of variables for a complex chemical process.¹ It is typically sparse and nonlinear. Description of this strategy is much easier than to implement it in practical software. Rather than tearing recycle streams and solving unit models in a modular fashion, an equation-oriented simulator assembles all the equations describing a process model together and solves them simultaneously.⁴ The key to the success of the approach is to start iterations from a good starting point. AspenPlus employs sequential modular calculation to initialize all variables and the switches to the EO solution methods.

The entire system of equations can be solved using an equation-solving package (simultaneous linearization) or the equations can be decomposed (partitioned) into a sequence of square partitions that may be solved independently using a structuring algorithm (Book and Ramirez, 1984; Ramirez, 1989).

In this study, we discuss process modeling and the primary interest in this study is the solution of chemical process flowsheeting (CPF) systems which are developed for use in the synthesis, design and optimization of steady-state chemical processes. There are subroutines for the flash unit, absorber and stripper. One constructs a complete process model by wiring up an appropriate set of building blocks.

Process description

The most widely used gas-treating process for acid gas removal in the natural gas and petroleum processing industries is the chemical solvent process, using various alkanolamines. The amines of proved commercial interest for acid gas removal by chemical absorption are monoethanolamine (MEA), diethanolamine (DEA), *N*-methyldiethanolamine (MDEA) and diisopropanolamine (DIPA).^{8–14}

Gas removal is a very important industrial operation, which has been described in many books; see e.g. Kohl and Nielsen (1997), Astarita *et al.* (1983), and Danckwerts (1970). The most widely used processes to sweeten natural gas are those using alkanolamines, and of the alkanolamines a common one is methyldiethanolamine (MDEA).^{9–10}

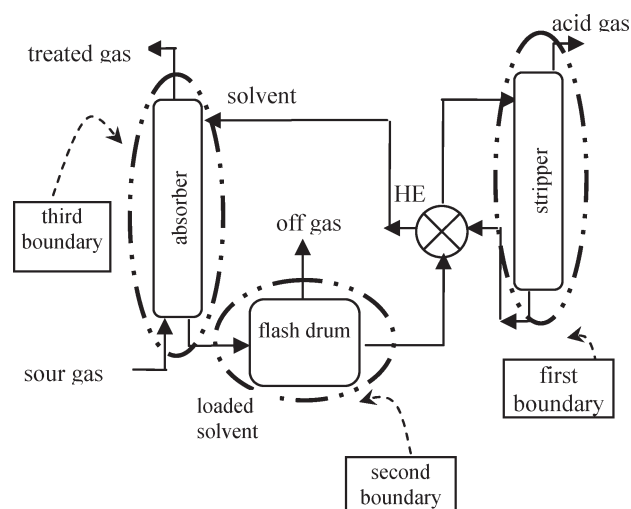


Fig. 1 – Illustration of an absorption/stripping system for the removal of acid gases

Absorption by a solvent is the technique most commonly used to process natural gas. The basic principle of the absorption process is illustrated in Fig. 1.

A sour gas containing H_2S and/or CO_2 is introduced at the bottom of a high-pressure absorber where it rises and counter-currently contacts an aqueous alkanolamine solution that is introduced at the top of the absorber. The loaded solvent can be flashed after leaving the washing tower to remove hydrocarbons possibly contained in the raw gas stream. That result is then pumped through heat exchangers where its temperature is raised. It is then introduced at the top of a stripper where it counter-currently contacts steam at an elevated temperature and reduced pressure. The steam strips the CO_2 and H_2S from the solution and the lean alkanolamine solution is pumped through the heat exchanger, where it is cooled, and reintroduced at the top of absorber.

Development of a mathematical model for steady state flowsheeting

Simultaneous-modular method

This approach is based on representing units as sets of equations. Of course, these equations must be provided by the user, selected from a model library or introduced as a new model to the simulator. To calculate a process flowsheet, all the equations describing all the unit operations present in the flowsheet are assembled and solved simultaneously by using standard numerical methods. The important considerations for this approach are size of the equation set, degree of freedom analysis and check for singularity, non-linearity of the equation

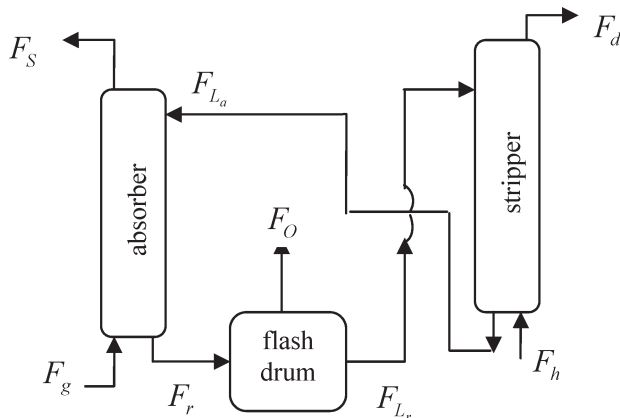


Fig. 2 – Simplified diagram of sweetening plant

set and the initialization for the set of unknown variables.

As seen from Fig. 2, there are three units, including absorber column, flash drum, and stripper. Mass balance around each unit is given by the following equations.

$$F_{g,i} + F_{L_{a,i}} - F_{s,i} - F_{r,i} = 0 \quad (1)$$

$i = \text{Cl}, \text{CO}_2, \text{H}_2\text{S}, \text{H}_2\text{O}$

$$F_{r,i} - F_{o,i} - F_{L_{r,i}} = 0 \quad (2)$$

$i = \text{Cl}, \text{CO}_2, \text{H}_2\text{S}, \text{H}_2\text{O}$

$$F_h + F_{L_r} - F_{L_a} - F_d = 0 \quad (3)$$

$i = \text{Cl}, \text{CO}_2, \text{H}_2\text{S}, \text{H}_2\text{O}$

In order to match the number of equations and unknowns, the following auxiliary equations are used:

$$F_{g,i} - \alpha_i F_{r,i} = 0 \quad (4)$$

$i = \text{Cl}, \text{CO}_2, \text{H}_2\text{S}, \text{H}_2\text{O}$

$$F_{L_{r,i}} - \beta_i F_{d,i} = 0 \quad (5)$$

$i = \text{Cl}, \text{CO}_2, \text{H}_2\text{S}, \text{H}_2\text{O}$

$$K_i F_{L_{r,i}} (F_{O,\text{CO}_2} + F_{O,\text{H}_2\text{S}} + F_{O,\text{Cl}} + F_{O,\text{H}_2\text{O}}) - F_{O,i} (F_{L_{r,\text{CO}_2}} + F_{L_{r,\text{H}_2\text{S}}} + F_{L_{r,\text{Cl}}} + F_{L_{r,\text{H}_2\text{O}}}) = 0 \quad (6)$$

$i = \text{Cl}, \text{CO}_2, \text{H}_2\text{S}, \text{H}_2\text{O}$

α_i, β_i are the efficiency of absorber and desorber. K_i is the k -Value of each component.

In this method, the amine circulation rate is constant.

Sequential-modular method

Our flowsheeting system allows us to build the model interactively using a computer workstation on which we can place icons for each type of unit and “wire” these icons together with streams. As

seen from Fig. 1, there are three boundaries, including absorber column, flash drum, stripper column corresponds to three modules.

The stream of lean MDEA to absorber is selected as tear stream because if this stream is teared the process is no longer of recycle type. After selection of tear stream topology, the process dictates the sequence of the calculations as (Absorber → Flash tank → Desorber). By selecting this stream as tear stream, we would be able to force the loop to have the desired value of lean MDEA.

To calculate absorber properties, stream variables values for the recycle stream are required. The recycle stream values are then calculated and checked against the values guessed for that iteration. If they agree within a tolerance, then the flowsheet is converged. If we assume the value of x for tear stream properties and calculate new value of $f(x)$ for it, the flowsheet is converged if we have $|f(x) - x| < a$ prescribed tolerance. A more general, weighted form is:

$$x^{k+1} = af(x^k) + (1-a)x^k \quad (7)$$

Which is useful if the iterations start to oscillate, e.g. $a = 0.5$. We can even accelerate the rate of convergence after two stages with the aid of the following equation:

$$x^{k+2} = x^{k+1} - \left[\frac{x^{k+1} - x^k}{f(x^{k+1}) - f(x^k)} \right] f(x^k) \quad (8)$$

Absorption and desorption columns

Absorption and desorption can be treated as a kinetically determined mass transfer process in which the degree of separation is determined by the mass and energy transfer rates between the phases being contacted on each tray. This approach allows dealing with ‘real’ trays right from the outset and it results in a physically more realistic model based on the fundamental chemistry and physics of the process. Two design approaches are in common use: the equilibrium-based approach, and the rate-based approach. The equilibrium-based approach is suitable for non-reactive systems. Equilibrium stage model assumes that the gas leaving the tray is in equilibrium with the liquid leaving the tray in a counter-current direction. More recently, a non-equilibrium stage (trayed columns) and a non-equilibrium continuous model (packed beds) have been developed. This non-equilibrium model may be solved numerically with a computer, which considers the actual trays or sections of packing and performs heat and material balances for each phase based on mass and heat transfer rates (Krishna-

murthy and Taylor, 1985). This type of modeling is often called the rate-based model.

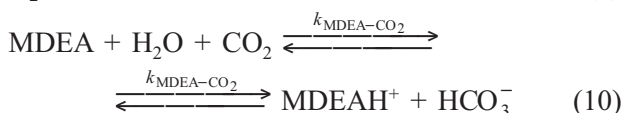
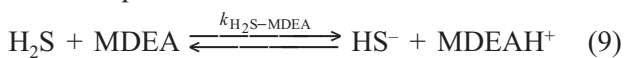
In the literature, several simulation studies of amine-based absorption of carbon dioxide are available. Some of them use simplified concepts, e.g. equal diffusivities (Glasscock, Critchfield, & Rochelle, 1991; Hagewiesche, Ashour Al-Ghawas, & Sandall, 1995) or enhancement factors (Sivasubramanian & Sardar, 1985; Tontiwachwuthikul, Meisen, & Lim, 1992; Pintola, Tontiwachwuthikul, & Meisen, 1993; Pacheco & Rochelle, 1998; Al-Baghli, Pruess, Yesavage, & Selim, 2001), other are restricted by the consideration of only one column stage or segment (Rascol, Meyer, & Prevost, 1996; Cadours & Bouallou, 1998).^{9–11}

Modern computer technology has made it possible to use sophisticated mass transfer rate-based models to design and simulate almost any type of gas treating systems (Katti, 1995; Katti and McDougal, 1986; Yu and Astarita, 1987; Krishnamurthy and Taylor, 1985; Sardar, 1985). Whereas, in designing and simulating real amine processes, data under stripping conditions are equally important. Furthermore, whatever little work has thus far been done on desorption or stripping from chemical solvent (Bosch *et al.*, 1990a, b; Glasscock *et al.*, 1991; Xu *et al.*, 1995), it has been done in isolation and there has never been a major attempt to investigate if the data collected under absorber conditions may be utilized to predict desorption rates.¹⁰

In this work, a model is suggested that balances gas and liquid phase separately and considers mass and heat transfer resistances according to the film theory by explicit calculation of the interfacial fluxes. The film model equations are combined with relevant reaction and diffusion kinetics, and include the specific features of electrolyte solutions. An important advantage of this model is that the hydrodynamics in the column can be directly involved via correlations for hold-up, pressure drop, interfacial area and mass transfer coefficients (Schneider *et al.*, 1999).

Chemical reactions

Methyldiethanolamine (MDEA) is today the most used tertiary amine for acid gas removal. The reaction between CO₂ and H₂S in MDEA solutions can be represented as:



The reaction between H₂S and MDEA is very fast and the reaction is considered instantaneous

with an infinite reaction rate, while the reaction with CO₂ is relatively slow. MDEA allows selective absorption of H₂S in the presence of CO₂, because of the reaction rate difference for CO₂ and H₂S with MDEA. When the correct additives/activators are used, MDEA offers several advantages over other amines also for bulk CO₂ removal. An important reason for this is the relatively low heat of absorption of CO₂ into MDEA solutions.

The reaction rate for CO₂ in a MDEA-solution can be calculated from:

$$-r_{\text{CO}_2-\text{MDEA}} = k_i c_{R_1 R_2 R_3 N} (c_{\text{CO}_2} - c_{\text{CO}_2,eq}) \quad (11)$$

Mass and energy balance

In this work, we simulated trayed columns. The mass transfer enhancement in gas/liquid systems is defined with respect to the absorption rate in gas/liquid systems. In two-phase gas/liquid systems, there is an interface with concentration gradients on both sides (Fig. 3).

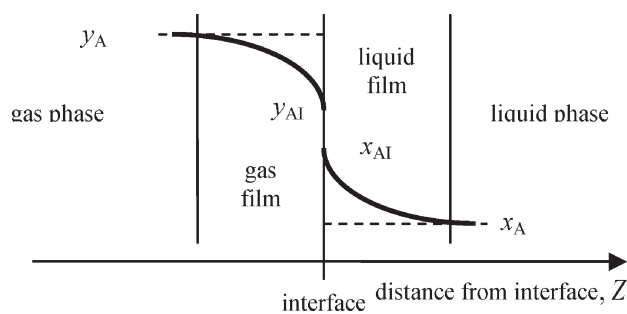


Fig. 3 – Concentration profile of solute A in the neighborhood of a gas-liquid interface

Taking the case of a gas mixture of A and B with a non-volatile liquid that absorbs only A, there are three resistances to the transport of species A from gas phase to liquid phase: in the gas phase, at the gas/liquid interface and in the liquid phase. The mole fraction in the bulk gas phase is y_A , which decreases to y_{AI} at the interface. In the liquid phase, the mole fraction starts at x_{AI} and falls to x_A . The interface resistance may be neglected in most operations, except in very high flux cases. It is assumed, that the concentrations at the interface are at steady state. The mole fractions y_{AI} and x_{AI} are then assumed to be in thermodynamic equilibrium, which is expressed by:

$$p_{i,int} = H_i c_{i,int} \quad (12)$$

$$\begin{aligned} F_{N,i,z} &= F_{g,in} y_{i,in} - F_{g,out} y_{i,out} = \\ &= k_{g,i} a (p_{i,out} - p_{i,int}) = k_{l,i} a E_i (c_{i,int} - c_{i,blk}) \quad (13) \end{aligned}$$

where $k_{g,i}$ and $k_{l,i}$ are the gas and liquid phase physical mass transfer coefficients of the solute gas

i , respectively. E_i is the enhancement factor of the dissolved gas i . The enhancement factor accounts quantitatively for the effect of reaction on mass transfer and it depends, among other, on the kinetic details of the particular reaction taking place.

$$E_i = \frac{-D_i \left(\frac{dc_i}{dZ} \right) \Big|_{Z=0} + r_i \Big|_{Z=0}}{k_l (c_{i,int} - c_{i,blk})} \quad (14)$$

For the system of CO₂-H₂S-MDEA, the overall mass transfer rates in the bulk of liquid on stage n of the column are given by the following equations:¹¹

$$D_{CO_2} \frac{d^2 c_{CO_2}}{dZ^2} + r_{CO_2-MDEA} = 0 \quad (15)$$

$$D_{H_2S} \frac{d^2 c_{H_2S}}{dZ^2} - D_{MDEA} \frac{d^2 c_{MDEA}}{dZ^2} - r_{MDEA-CO_2} = 0 \quad (16)$$

$$D_{HCO_3^-} \frac{d^2 c_{HCO_3^-}}{dZ^2} - r_{MDEA-CO_2} = 0 \quad (17)$$

$$D_{HS^-} \frac{d^2 c_{HS^-}}{dZ^2} + D_{MDEA} \frac{d^2 c_{MDEA}}{dZ^2} + r_{MDEA-CO_2} = 0 \quad (18)$$

$$D_{MDEAH^+} \frac{d^2 c_{MDEAH^+}}{dZ^2} + D_{MDEA} \frac{d^2 c_{MDEA}}{dZ^2} = 0 \quad (19)$$

$$K_{H_2S-MDEA} \left(c_{H_2S} \frac{d^2 c_{MDEA}}{dZ^2} + c_{MDEA} \frac{d^2 c_{H_2S}}{dZ^2} + \right. \\ \left. + 2 \frac{dc_{H_2S}}{dZ} \frac{dc_{MDEA}}{dZ} \right) - \\ \left(c_{HS^-} \frac{d^2 c_{MDEAH^+}}{dZ^2} + c_{MDEAH^+} \frac{d^2 c_{HS^-}}{dZ^2} + \right. \\ \left. + 2 \frac{dc_{HS^-}}{dZ} \frac{dc_{MDEAH^+}}{dZ} \right) = 0 \quad (20)$$

The boundary conditions are as follows:

At $Z = \delta_l$ (edge of the liquid film):

$$c_i = c_{i,blk} \quad (21)$$

($i = CO_2, H_2S, MDEA, MDEAH^+, HCO_3^-, HS^-$)

At $Z = 0$ (gas-liquid interface):

$$F_{g,in} y_{CO_2,in} - F_{g,out} y_{CO_2,out} - \\ - E_{CO_2} a k_{l,CO_2} (c_{CO_2} \Big|_{Z=0} - c_{CO_2,blk}) = 0 \quad (22)$$

$$F_{g,in} y_{H_2S,in} - F_{g,out} y_{H_2S,out} - \\ - E_{H_2S} a k_{l,H_2S} (c_{H_2S} \Big|_{Z=0} - c_{H_2S,blk}) = 0 \quad (23)$$

$$\frac{dc_{HCO_3^-}}{dZ} = 0 \quad (24)$$

$$D_{MDEA} \frac{dc_{MDEA}}{dZ} + D_{HS^-} \frac{dc_{HS^-}}{dZ} = 0 \quad (25)$$

$$D_{MDEA} \frac{dc_{MDEA}}{dZ} + D_{MDEAH^+} \frac{dc_{MDEAH^+}}{dZ} = 0 \quad (26)$$

$$K_{H_2S-MDEA} c_{H_2S} c_{MDEA} - c_{HS^-} c_{MDEAH^+} = 0 \quad (27)$$

The temperature on the plate is determined from an enthalpy balance around the plate:

$$A_n T^{n-1} + B_n T^n + C_n T^{n+1} = D_n \quad (28)$$

That:

$$A_n = F_L^{n-1} c_{p,L}^n \quad (29)$$

$$B_n = -[F^n c_{p,G}^n + F_L^n c_{p,L}^n] \quad (30)$$

$$C_n = [F^{n+1} c_{p,G}^{n+1}] \quad (31)$$

$$D_n = \phi_{loss} - \phi_{abs} - \phi_{reac} \quad (32)$$

Where c_p is the average molar heat for each streams. ϕ_{loss} is heat loss or cooling load of plate and ϕ_{abs} is total heat of absorption and ϕ_{reac} is total heat released by reaction.

Method of solution

Here, we will only address the calculations related to steady-state simulation, which is represented by a mathematical model consisting of a set of algebraic equations. The more complex case of distributed or dynamics models (with partial differential equations) also are not discussed; nevertheless, the principle of the solution approach described below can be applied to simulation problems involving distributed models. The mathematical model represents only mass and energy balance equations.

The solution approach needs to address the following issues:

- Simulation approach (method of solution)
 - Flowsheet decomposition
 - Equation ordering
 - Convergence technique (solution of algebraic equations)
- Simulation strategy.

Simultaneous-modular method

Application of the simultaneous-modular method for the loop of plant provides 31 equations with 31 unknowns. These equations resulted from expansion of eqs. (1–6) when applied for all components presented in the plant. A mathematical solver code is employed to solve the existing system of equations for the entire cycle by the Newton global convergence method. The main program and subroutines of this solver are adapted from FORTRAN Powerstation which is a popular programming language and has acceptable speed for tedious numerical calculations. In the assembled algebraic equation set, there are some auxiliary definitions for separation equipment including absorber and desorber. These definitions are provided for each component as follows:

$$\eta_i = \frac{\Sigma(F x_i)_{exit}}{\Sigma(F x_i)_{entrance}} \quad (33)$$

F in eq. 33 stands for the mole flow rate value of any stream in the plant and x_i is mole fraction of each component in the stream.

With the aid of the first calculation iteration results, we are able to predict the efficiencies and K -values more precisely. Having estimated composition of liquid and gas phase, K -values are then recalculated by application of the NRTL activity model for liquid phase and Peng-Robinson equation of State in the gas phase. The flow diagram of the calculating process is presented in Fig. 4.

Sequential modular method

Mathematical model is developed for a simplified sweetening loop. Schematic of this unit is in Fig. 2. The modular structure of the code is based on unit subroutines containing the governing equations for the system's components. A main program calling these subroutines links the components together according to the cycle diagram. Property subroutines contained in a separate database serve to provide thermodynamic properties of the gas and liquid.

For each set of calculations, we first select a composition for lean MDEA stream. At this moment, we are not sure of the composition of this stream but we only want to force the loop to have a specified amount of MDEA in lean MDEA. While iterations are performed in prescribed sequences, the calculated composition of the tear stream is affected by the performance of equipment changes.

Because the plant consists of units mainly including absorber, flash tank and stripper, and because the working fluid can have different conditions, the code is built upon unit subroutines in separate modules. Each time we bring a unit into our calculation sequences, the unit is simulated by its

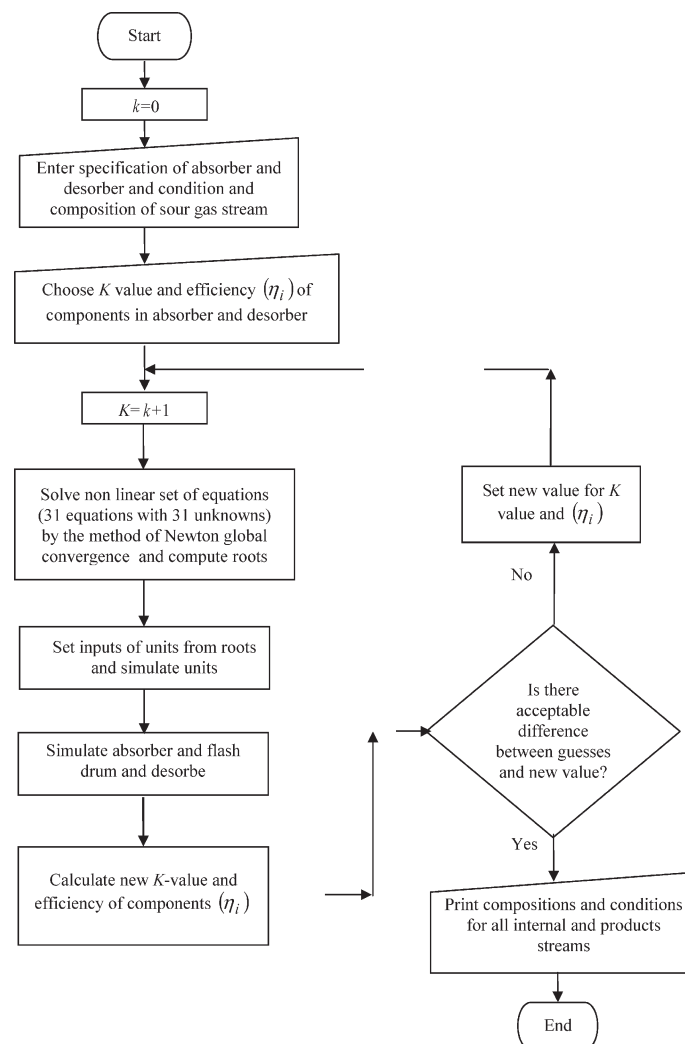


Fig. 4 – Flow diagram of the calculating process in simultaneous-modular method

private subroutine in a separate module containing the physical equations required to fully describe its behavior, such as energy balance, conservation of mass for each material species, heat and mass transfer and thermodynamic equilibrium. The input of the program specifies operating conditions.

Results and discussion

The developed model was tested on experimental data of an industrial plant. Representative input conditions for the acid gas absorber and desorber in a plant are summarized in Table 1.

In order to verify that the model developed in this work accurately represents the reactive absorption/desorption process, a detailed examination was conducted in which model equations were solved numerically for each system and for each set of operating conditions. Number of trays is from the bottom to the top of the column. Detailed results of se-

quential and simultaneous modular methods as well as operating data are given in Tables 2–4 for all streams. These tables indicate relatively better model results for the simultaneous modular method. Therefore, the performance of the plant is investigated with this method.

As may be seen from Fig. 5, the flow rate of the gas exiting the flush drum is increased with the increased amine circulation rate. In addition to the chemical absorption, physical absorption also is done in the absorption tower. Therefore, hydrocarbons are absorbed physically. Methane has higher absorption than other hydrocarbons. In addition, acid gases and water have little physical absorption. With entering a higher amount of amine, absorption ability increases and physical absorption increases. However, these absorbed gases leave the amine in the flush drum by changing the pressure of the system.

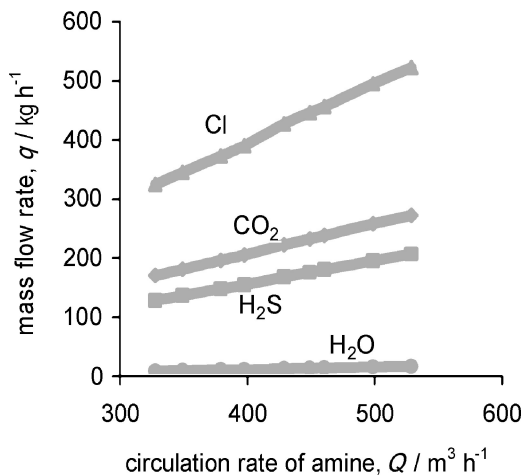


Fig. 5 – Influence of amine circulation rate on the flow rate of gas exiting the flush drum

Fig. 6 shows the variation of acid gas compositions in sweet gas against amine circulation rate.

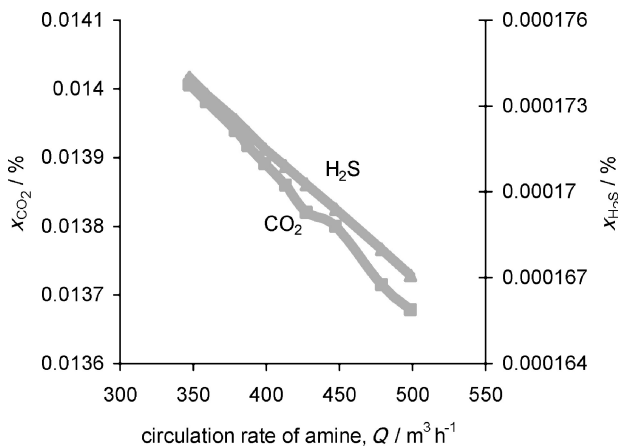


Fig. 6 – Influence of amine circulation rate on acid gas composition in sweet gas

Table 1 – Properties of streams entering the absorber unit

	Lean amine	Sour gas
mass flow rate, $q/\text{kg h}^{-1}$	463152	138010
temperature, $\vartheta/^\circ\text{C}$	53	21
pressure, p/kPa	7580	7401
mole fraction, $x_{\text{H}_2\text{O}}/\%$	91.89	0.03
mole fraction, $x_{\text{CO}_2}/\%$	–	6.41
mole fraction, $x_{\text{H}_2\text{S}}/\%$	–	3.85
mole fraction, $x_{\text{Cl}}/\%$	–	89.71
mole fraction, $x_{\text{MDEA}}/\%$	8.11	–

Table 2 – Comparison of calculated and industrial data for lean amine circulation rate

	Industrial data	Sequential modular method	Simultaneous-modular method
mass flow rate, $q/\text{kg h}^{-1}$	18469.49	18186	18709
temperature, $\vartheta/^\circ\text{C}$	53	50	51.5
pressure, p/kPa	7580	7511	7522
mole fraction, $x_{\text{H}_2\text{O}}/\%$	91.89	89.98	91.99
mole fraction, $x_{\text{MDEA}}/\%$	8.11	10.01	8

Table 3 – Comparison of calculated and industrial data for sweet gas

	Industrial data	Sequential modular method	Simultaneous-modular method
mass flow rate, $q/\text{kg h}^{-1}$	6502.2	6325	6433
temperature, $\vartheta/^\circ\text{C}$	56	54	55.2
pressure, p/kPa	7290.8	7289.9	7289.99
mole fraction, $x_{\text{H}_2\text{O}}/\%$	0.29	0.32	0.3
mole fraction, $x_{\text{Cl}}/\%$	99.70	99.67	99.69
mole fraction, $x_{\text{CO}_2}/\%$	0.01	0.011	0.00965
mole fraction, $x_{\text{H}_2\text{S}}/\text{ppm}$	4	3.5	3.5

Table 4 – Comparison of calculated and industrial data for stripped gas from desorber

	Industrial data	Sequential modular method	Simultaneous-modular method
mass flow rate, $q/\text{kg h}^{-1}$	2265.99	2326	2213.74
temperature, $\vartheta/^\circ\text{C}$	103	102.2	102.5
pressure, p/kPa	170	172.1	171
mole fraction, $x_{\text{H}_2\text{O}}/\%$	66.60	67.82	65.98
mole fraction, $x_{\text{Cl}}/\%$	0.31	0.3	0.32
mole fraction, $x_{\text{CO}_2}/\%$	20.67	19.17	21
mole fraction, $x_{\text{H}_2\text{S}}/\%$	12.42	12.71	12.7

Further increase of the amine circulation rate will cause the absorption ability to increase. In addition, acid gases are transferred to liquid phase by higher absorption rate. Therefore, the amount of these gases is decreased in sweet gas.

The effect of concentration of MDEA on the specific rates of absorption of CO_2 and H_2S are shown in Fig. 7. MDEA is a tertiary amine with very low reactivity, where the absorption rate at the given conditions increases from MDEA, while that of H_2S increases to a much lesser extent. At low concentration of MDEA, CO_2 and H_2S compete to react with MDEA and when concentration of MDEA increases to about $c = 2.5 \text{ kmol m}^{-3}$ they can absorb into MDEA to a greater extent without tough competition with each other.

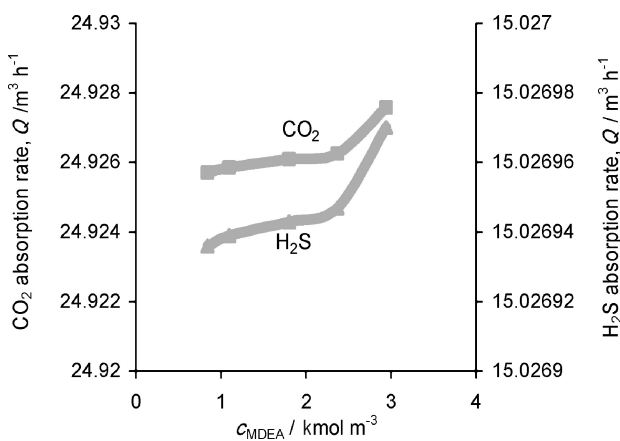


Fig. 7 – Variation of absorption rate of CO_2 , H_2S in liquid phase vs. c_{MDEA} in stripper

Resulting concentration profiles of various species in the liquid film of stripper were plotted as shown in Fig. 8.

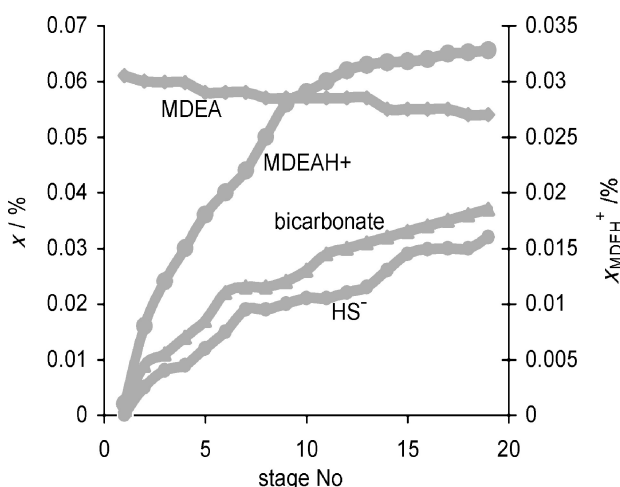


Fig. 8 – Variation of liquid phase compositions vs. stage number in stripper

Concentration profiles for individual species were found to follow expected trends. No unusual or unexpected behavior was observed, indicating that our theoretical and numerical approach to modeling reactive process over a hemispherical film was right. In the liquid film, decomposition of bicarbonate, MDEAH^+ , HS^- will cause the H_2O and MDEA to produce. Therefore, composition of water and amine will increase and HCO_3^- , HS^- , MDEAH^+ will decrease when the liquid flows down the column. Also, condensation of H_2O from gas phase to liquid and production of H_2O from reaction will increase the water in the liquid phase.

Fig. 9 also shows variation of mole fraction of CO_2 , H_2S and H_2O in gas stream against stage number in stripper. As the liquid flows down the tower, it continues to desorb acid gases. Acid gas is transferred to gas phase from liquid phase and H_2O vapor is condensed to liquid phase, which causes variation of the mole fraction. As may be seen, the mole fraction of CO_2 , H_2S increases during the tower. Temperature of liquid phase drops down during the column from down to up. Also, vapor pressure of water decreases. Thus, the mole fraction of H_2O is decreased.

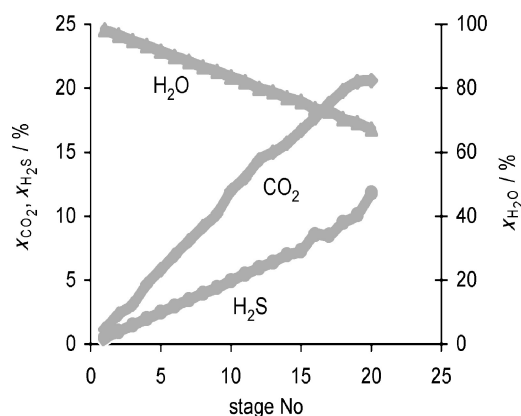


Fig. 9 – Variation of stripped gas compositions vs. stage number in stripper

As seen from Fig. 10, the CO_2 enhancement factors are close to unity for the MDEA system. This indicates that the CO_2 reaction with the MDEA occurs in the liquid bulk. Therefore, the process of CO_2 absorption with MDEA is controlled only by the physical diffusion of CO_2 in the liquid film. The H_2S enhancement factor is of magnitude unity at bottom of absorber. The extreme variation of the H_2S enhancement factors along the absorbers results from the interaction of H_2S with CO_2 . This interaction is quantified by the numerical solution of the governing differential equations. The extraordinary trends obviously cannot be obtained from simple analytical enhancement factor expressions.

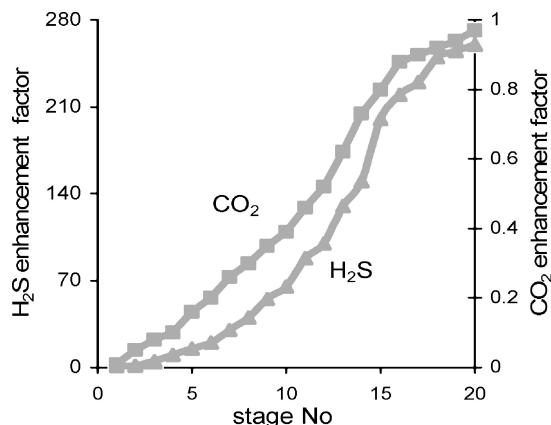


Fig. 10 – Variation of H_2S , CO_2 enhancement factor profile vs. stage number in absorber

In Fig. 11, variation of mole fraction of CO_2 and H_2S in outlet gas stream in absorption column is shown. As can be seen from this figure, with increasing stage number, the acid gas concentrations decreased. Reaction of CO_2 and H_2S occurs in the liquid phase and the liquid is flowed down the column. Thus, acid gases transfer to liquid phase. Absorption mechanism of CO_2 and H_2S is different. The backward rate of the reaction between CO_2 and amine is small and CO_2 absorption is low. The high concentration of the acid gases in addition to the scarcity of the amines in the bottom makes the competition between CO_2 and H_2S to react with the amines extremely difficult. Due to the instantaneous reaction that occurs between H_2S and the amines, H_2S absorption is high and H_2S consumes most of the amines present, leaving a negligible amount to react with CO_2 . The absorption of H_2S is limited by the equilibrium, which is governed by the inlet liquid stream H_2S loading and temperature in addition to the molarity of the alkanolamine and the system pressure. Therefore, any degree of purification of H_2S in the absence of other acid gases may be reached easily by adjusting these variables.

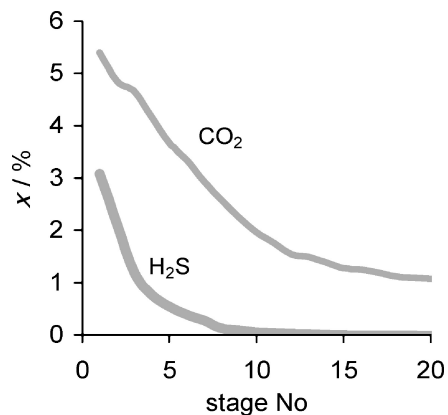


Fig. 11 – Variation of mole fraction of CO_2 and H_2S in the outlet gas stream vs. absorber stage number

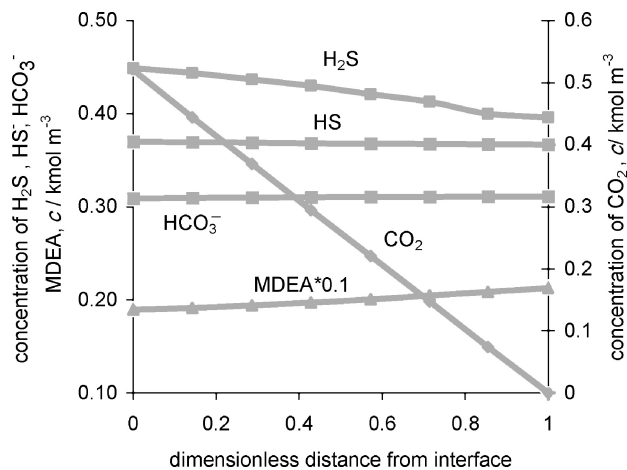


Fig. 12 – Predicted concentration profiles for CO_2 , H_2S absorption in aqueous MDEA solution

The liquid film concentration profiles of the reacting species at the top of the absorber are shown in Fig. 12. The concentrations of MDEA and ions, as seen from these plots, increase from interface to bulk of liquid, but the concentrations of CO_2 and H_2S decrease. CO_2 and H_2S absorb from gas to liquid and in the interface we have maximum concentration.

Conclusion

The model presented in this work accurately predicted sweetening performance when the results were compared with operating data. Calculated and industrial data for both internal and external streams are in good agreement according to the simplicity of the model, especially in the simultaneous modular method. Thus, the suggested model can be regarded as predictive in a wide range. A sequential modular approach flowsheeting was used to simulate a commercial sweetening plant. Before flowsheeting of the sweetening plant, the three main equipment of sweetening plant (absorber, flash drum and stripper) were simulated in rigorous manner. A rigorous rate-based model for reactive absorption and desorption by aqueous MDEA amine is suggested. This model is based on the two-film theory and considers the acceleration of mass transport due to a complex system of chemical reactions without using simplified enhancement factor concepts. The precise description of the accelerating effort is established via the implementation of liquid film reactions. The latter allows for the calculation of non-linear concentration profiles within the liquid film.

ACKNOWLEDGEMENT

The financial support of this work by the Iranian Oil and Gas Company is appreciated.

Nomenclature

a	– total area of the gas-liquid interface, m^2
c	– concentration, $kmol\ m^{-3}$
c_p	– molar heat capacity, $J\ mol^{-1}\ K^{-1}$
D	– diffusivity, $m^2\ s^{-1}$
E	– enhancement factor
F_g	– gas mole flow rate, $kmol\ s^{-1}$
F_N	– molar flow rate of the solute gas, $kmol\ h^{-1}$
F_O	– molar flow rate of stripped gas, $kmol\ h^{-1}$
H	– Henry's constant, $kPa\ m^3\ kmol^{-1}$
J	– mole flux, $kmol\ m^{-2}\ K^{-1}$
K	– reaction equilibrium constant
$k_{g,i}$	– gas phase physical mass transfer coefficients of the solute gas, $kmol\ m^{-2}\ s^{-1}\ kPa^{-1}$
k_i	– K value
k_l	– reaction rate constant, $L\ mol^{-1}\ s^{-1}$
$k_{l,i}$	– liquid phase physical mass transfer coefficients of the solute gas, $m\ s^{-1}$
p	– pressure, kPa
q	– mass flow rate, $kg\ h^{-1}$
Q	– volume flow rate, $m^3\ h^{-1}$
r	– reaction rate, $mol\ L^{-1}\ s^{-1}$
T	– temperature, K
x	– mole fraction of component in liquid stream, %
y	– mole fraction of component in gas stream
Z	– distance in the liquid film, m

Greek letters

η	– efficiency
δ	– film thickness, m
ϕ	– heat flow rate, $kJ\ min^{-1}$
ϑ	– temperature, $^{\circ}C$

Subscripts

blk	– liquid bulk
g	– gas phase
i	– component i
in	– going to stage
int	– interface

out – leaving stage

l – liquid phase

References

1. Lory, P., *Methods & Applications* **30** (1997) 4965.
2. Gani, R., Hostrup, M., *Computer Aided Process Engineering*, Institut for Kemiteknik Danmarks Tekniske Universitet, September, Denmark, 1999.
3. Kisala, T. P., Trevino-Lozano, R. A., Boston, J. F., Britt, H. I., Evans, L. B., *Comp. Chem. Eng.* **11** (6) (1987) 567.
4. Westerberg, A., Piela, P. C., *Equation-Based Process Modeling*, Department of Chemical Engineering, and the Engineering Design Research Center, Pittsburgh, August 1994.
5. Barton, P. I., *The Equation Oriented Strategy for Process Flowsheeting*, Department of Chemical Engineering, Massachusetts Institute of Technology, March 2000.
6. Ercal, F., Book, N. L., Pait, S., Fielding J. J., *Comp. Chem. Engng.* **19** (1995) 91.
7. Sargent, R. W. H., Westerberg, A. W., *Trans. Inst. Chem. Engrs.* **12** (1964) 190.
8. Kucka, L., Mullerb, I., Kenig, E. Y., Gorak, A., *Chem. Eng. Science* **58** (2003) 3571.
9. Pacheco, M. A., Rochelle, G. T., *Ind. Eng. Chem. Re.* **37** (1998) 4107.
10. Bolhar-Nordenkamp, M., Friedl, A., Koss, U., Tork, T., *Chem. Engng. and Processing* **43** (2004) 701.
11. Al-Baghli, N. A., Pruess, S. A., Yesavage, V. F., Selim, M. S., *Fluid Phase Equilibria* **185** (2001) 31.
12. Solbraa, E., *Equilibrium and Non-Equilibrium Thermodynamics of Natural Gas Processing*, Thesis, December 2002.
13. Buzek, J., Jaschik, M., Podkanski, J., Wasilewsk, W., Mrozowski, J., *Chem. Engng & Processing* **37** (1998) 233.
14. Jamal, A., Meisen, A., Lim, C. J., *Chem. Engng. Sci.* **61** (2006) 6571.
15. Benjamin, A. A., Westerberg, A. W., *Compiling and solving 100,000 equations on a PC in (3) minutes*, INFORMS Meeting, Montreal, Quebec, Canada, April 28, 1998.
16. Piela, P., McKelvey, R., Westerberg, A., *J. Manag. Inf. Sys.* **9** (1993) 91.
17. Robertson, J. L., Subrahmanian, E., Thomas, M. E., Westerberg, A. W., *Management of the Design Process: The Impact of Information Modeling*, invited paper at Foundations of Computer Aided Process Design Conference, Snowmass, CO, USA (1994).
18. Westerberg, A. W., Dean, R. B., *Computers and Chemical Engineering* **9** (5) (1985) 517.